Published in final edited form as:
ACS Chem Biol. 2009 November 20; 4(11): 915–927. doi:10.1021/cb900146k.

Design and Antimicrobial Action of Purine Analogs that Bind Guanine Riboswitches

Jane N. Kim[‡,†], **Kenneth F. Blount**[‡,†,§], **Izabela Puskarz**[‡,§], **Jinsoo Lim**[‡,§], **Kristian H. Link**[‡,¶], and **Ronald R. Breaker**[‡,¶,#,*]

[‡]Department of Molecular, Cellular and Developmental Biology, Yale University, P.O. Box 208103, New Haven, Connecticut 06520-8103, USA

[¶]Howard Hughes Medical Institute, Yale University, P.O. Box 208103, New Haven, Connecticut 06520-8103, USA

[#]Department of Molecular Biophysics and Biochemistry, Yale University, P.O. Box 208103, New Haven, Connecticut 06520-8103, USA

Abstract

Riboswitches are structured RNA domains that can bind directly to specific ligands and regulate gene expression. These RNA elements are located most commonly within the noncoding regions of bacterial mRNAs, although representatives of one riboswitch class have been discovered in organisms from all three domains of life. In several Gram positive species of bacteria, riboswitches that selectively recognize guanine regulate the expression of genes involved in purine biosynthesis and transport. Because these genes are involved in fundamental metabolic pathways in certain bacterial pathogens, guanine-binding riboswitches may be targets for the development of novel antibacterial compounds. To explore this possibility, the atomic-resolution structure of a guanine riboswitch aptamer from *Bacillus subtilis* was used to guide the design of several riboswitch-compatible guanine analogs. The ability of these compounds to be bound by the riboswitch and repress bacterial growth was examined. Many of these rationally designed compounds are bound by a guanine riboswitch aptamer *in vitro* with affinities comparable to that of the natural ligand, and several also inhibit bacterial growth. We found that one of these antimicrobial guanine analogs (6-*N*-hydroxylaminopurine, or G7) represses expression of a reporter gene controlled by a guanine riboswitch in *B. subtilis*, suggesting it may inhibit bacterial growth by triggering guanine riboswitch action. These studies demonstrate the utility of a three-dimensional structure model of a natural aptamer to design ligand analogs that target riboswitches. This approach also could be implemented to design antibacterial compounds that specifically target other riboswitch classes.

[*]Corresponding author, ronald.breaker@yale.edu, Phone: (203) 432-9389, Fax: (203) 432-0753.
[†]These authors contributed equally to this work.
[§]Current address for K.F.B and I.P. is BioRelix, Inc., 5 Science Park, New Haven, CT 06511. Current address for J.L. is Idenix Pharmaceuticals, Inc., 60 Hampshire Street, Cambridge, MA 02139,

INTRODUCTION

Currently used antibiotics act on only a few cellular processes (1–3), and bacteria are steadily becoming resistant to known drugs (4, 5). Common classes of antibiotics bind to diverse targets, including enzymes in the folic acid biosynthesis pathway (6), cell wall biosynthesis components (7), DNA topoisomerase enzymes (8), and ribosomes (9). However, novel antibacterial agents that affect different cellular systems are needed to combat emerging antibiotics-resistant bacteria. Unfortunately, it is challenging to identify critical processes and pathways that are sufficiently widespread and conserved to permit the development of broad-spectrum antibiotics.

The involvement of ribosomes in the mechanisms of antibacterial agents is intriguing because they carry the only noncoding RNAs that are targeted by commercial antibiotics. However, numerous classes of noncoding RNAs are being discovered in bacteria (10), which may offer new RNA-based targets for antibacterial compound development. We have been particularly interested in determining whether riboswitches (11–15) could act as such targets.

Riboswitches are structured RNA elements that are usually located in the 5′ untranslated regions (UTRs) of bacterial mRNAs, though plant and fungal riboswitches have also been characterized (16–20). Riboswitches selectively bind to small molecules, and ligand binding typically results in the regulation of genes that are involved in the biosynthesis or transport of the cognate ligand. Each riboswitch class generally consists of two regions, an aptamer domain and an expression platform. The aptamer is a conserved, structured receptor that selectively recognizes the ligand. The expression platform adopts different folded conformations depending on the occupation state of the aptamer, and the structure of the expression platform ultimately establishes whether the associated genes are expressed.

Most known riboswitches are involved in feedback control wherein the build-up of an essential metabolite triggers the down-regulation of genes whose protein products make or import more of the metabolite. In these cases, it is predicted that analogs of the natural ligand could bind to a riboswitch and cause repression of genes necessary for maintaining an adequate concentration of the metabolite. Riboswitch-mediated repression of genes necessary to synthesize or import essential metabolites may cause inhibition of bacterial growth or even cause bacterial cell death.

Previous studies have examined the potential utility of several riboswitch classes as antibacterial drug targets (21). For example, the thiamin pyrophosphate (TPP) analog pyrithiamine pyrophosphate binds to TPP riboswitches *in vitro* (22–25) and can inhibit bacterial and fungal growth, likely at least in part by binding to TPP riboswitches and repressing the expression of thiamin biosynthesis and transport genes (26–30). Also, lysine analogs such as L-aminoethylcysteine (AEC) and DL-4-oxalysine are known to bind to lysine riboswitches and repress gene expression of riboswitch-controlled genes (31, 32). However, the antimicrobial effects of compounds such as AEC may also be caused by their incorporation into proteins (33). Furthermore, it was recently discovered that the flavin mononucleotide (FMN) analog roseoflavin can bind to an FMN riboswitch *in vitro* (21, 34,

35), and possibly inhibits *B. subtilis* growth by repressing the expression of genes controlled by FMN riboswitches (35, 36). Other riboswitch classes also regulate fundamental metabolic pathways (11–15), and thus have the potential to become antibiotic targets. One example is the guanine riboswitch class (37), which also has one of the most highly characterized three-dimensional structures (38–44), making it an ideal candidate for structure-based drug design.

RESULTS AND DISCUSSION

Guanine Riboswitch-controlled Genes in *B. SUBTILIS*

Guanine riboswitches are found in several Gram positive species of bacteria, including the pathogens *Bacillus anthracis* and *Staphylococcus aureus* (37, 45). Often, as in the case of the *xpt-pbuX* guanine riboswitch in *B. subtilis* (Figure 1, panel a), a guanine riboswitch forms a transcription terminator stem in response to ligand binding and thereby represses the expression of the downstream gene or set of genes. *B. subtilis* carries four highly-conserved guanine riboswitches that collectively regulate the expression of the purine transport and metabolism genes *xpt-pbuX*, *pbuG*, and *nupG* (formerly named *yxjA*) (46) as well as the 12-gene operon responsible for *de novo* purine biosynthesis (*pur* operon) (Figure 1, panel b). The level of conservation among these four riboswitch aptamers suggests that a compound could be designed to bind to all of them. Thus, although none of the genes associated with this riboswitch have been identified as individually essential for survival (47), the combined effect of suppressing expression of all of the associated genes may impede purine metabolism and transport sufficiently to be deleterious to bacterial replication or viability.

To test whether simultaneously repressing all of the guanine riboswitch-controlled genes would be deleterious to *B. subtilis*, we systematically deleted all of these transcriptional units, except for the *pur* operon. For this operon, the region of the genome encompassing the promoter and the riboswitch element was replaced with a xylose-inducible promoter (Pxyl) (35, 48). In the absence of xylose, the growth rate of this conditional knockout strain (Figure 1, panel c) in Luria-Bertani (LB) medium was reduced compared to a wild-type strain, demonstrating that repression of the guanine riboswitch-controlled genes indeed results in slower growth. Under these growth conditions, quantitative reverse transcription and polymerase chain reaction (RT-PCR) amplification of the *pur* operon transcript revealed that a low level of transcript is present in the population of cells even in the absence of xylose (data not shown). This suggests that complete growth inhibition was not observed due to the low level of *pur* operon expression, which would maintain a low level of *de novo* purine biosynthesis.

Repeated attempts to delete the *pur* operon entirely in a *xpt-pbuX*, *pbuG*, *nupG* triple knockout strain were unsuccessful, suggesting that the simultaneous repression of all of these gene products may completely inhibit bacterial growth. These observations are consistent with our hypothesis that a novel compound designed to selectively target guanine riboswitches could inhibit *B. subtilis* growth. However, it is important to note that guanine-mediated repression of gene expression by purine riboswitch action may still permit low amounts of gene expression (37, 42), and therefore our gene deletion experiments may not perfectly mimic the cellular effects of analogs that trigger riboswitch action.

Guanine Analogs are Bound by Guanine Riboswitch Aptamers

Guanine riboswitch aptamers fold to form a three-stem junction from which the three base-paired stems P1, P2 and P3 radiate (37) (Figure 1, panel a). For the *xpt-pbuX* riboswitch from *B. subtilis* (hereafter termed the *xpt* riboswitch), the formation of the P1 helix is stabilized by the binding of guanine, allowing a terminator structure to form in the expression platform. In the absence of ligand, the 3′ shoulder of P1 can base pair with a region of the expression platform to form an antiterminator hairpin, thereby preventing the formation of the terminator and allowing transcription of the open reading frame (ORF) to proceed. Many nucleotides within the two hairpin loops L2 and L3 are highly conserved, and the loops interact both in the presence or absence of ligand to aid the process of ligand recognition (43, 44). Similarly, most of the nucleotides in the junction region of the aptamer are highly conserved and are also involved in ligand recognition. When the ligand is absent, the nucleotides of the junction region are relatively disordered, whereas in the presence of guanine, these nucleotides assemble into a tight binding pocket (37–39).

The three-dimensional structure of the *xpt* riboswitch aptamer from *B. subtilis* bound to guanine illustrates that the ligand is almost completely enveloped by nucleotides of the aptamer core (Figure 2, panel a) (38, 39). The aptamer makes several contacts with the ligand, and seven intermolecular hydrogen bonds are formed. The relative binding affinities for numerous guanine analogs are consistent with this model for intimate ligand recognition (37). Notably, one of the cytosine residues of the riboswitch junction region (C74) (Figure 1, panel a) forms a Watson-Crick pairing interaction with the guanine ligand. Mutation of C74 to a uridine residue renders the riboswitch unresponsive to guanine (49), reflecting its crucial role in ligand recognition.

Examination of the three-dimensional structure of the *xpt* aptamer also reveals two regions of the binding pocket wherein functional group modifications of guanine should be accommodated without large adverse effects on the binding interaction. These regions surround the C2 and C6 positions of the guanine ligand (Figure 2, panel b). We therefore predicted that additional functional groups could be added to C2 or C6 with minimal deleterious effects on ligand binding. To test this hypothesis, a collection of C2- or C6-modified guanine analogs were obtained or synthesized (Figure 3, panel a) and their ability to bind to the riboswitch and inhibit bacterial growth was assessed (Figure 3, panel b).

In-line probing assays (50) were performed with the *xpt* aptamer to assess the changes caused by these analogs on the structure of the aptamer, and to derive the apparent dissociation constant (K_D) for analog binding. In-line probing assays exploit the fact that internucleotide linkages in unstructured regions of RNA usually undergo more rapid spontaneous internal phosphoester transfer compared to linkages in structured regions. Internal phosphoester transfer involving nucleophilic attack by a 2′-oxygen atom on the adjoining phosphorus center results in chain cleavage. As the secondary or tertiary structures of a riboswitch aptamer change with addition of ligand, some internucleotide linkages change both their structural context and their susceptibility to spontaneous cleavage. The differences in RNA degradation products can be visualized via polyacrylamide agarose gel

electrophoresis (PAGE) and evaluated to determine the locations of RNA shape changes and to estimate K_D values for ligand-RNA complexes (50, 51).

An in-line probing assay using the *xpt* aptamer (Figure 1, panel a) from *B. subtilis* was used to assess whether each guanine analog at a concentration of 1 μM causes modulation of aptamer structure. Indeed, the majority of the analogs induce changes in spontaneous cleavage of the *xpt* aptamer to yield a pattern of RNA cleavage products similar to that observed when guanine is added to the reaction (data not shown). Even compounds that induce little or no structural modulation at 1 μM exhibit binding at higher ligand concentrations (Figure 3, panel a). Equilibrium dissociation constant (K_D) values for the analogs were determined by conducting in-line probing assays at various concentrations of each compound as depicted for G7 (Figure 3, panel b). K_D values observed range from 500 pM to 3.3 μM, with one of the analogs (G4) exhibiting better binding affinity for the riboswitch than guanine (K_D ~ 5 nM) (37). These findings indicate that new chemical groups can be added at the C2 and C6 positions of guanine without completely disrupting the RNA-ligand binding interaction, and in some instances can improve binding.

Inhibition of Bacterial Growth by Riboswitch-binding Guanine Analogs

Each of the compounds tested for guanine riboswitch binding were assessed for the ability to inhibit bacterial growth. *B. subtilis* cultures were grown for 10 hours at 37°C in glucose-minimal medium (GMM) in the presence of 100 μM of each compound separately (Figure 4, panel a). Under these conditions, five of the analogs cause greater than 50% inhibition of cell growth as measured by OD_{600}. Antimicrobial susceptibility testing (52) revealed that G6, G7 and G15 completely inhibit growth for 24 hours in GMM when concentrations of analog are above the minimum inhibitory concentration (MIC) (Figure 4, panel b). Although G6 exhibits an MIC in the low micromolar range (3.9 μM), the MICs for G7 and G15 are relatively high (260 μM and 500 μM, respectively) compared to commonly used antibacterial agents (52). Moreover, the MICs for G6, G7 and G15 are higher in a rich medium (LB). These findings indicate that exogenous nutrients present in rich medium, which include natural purine metabolic intermediates, can offset the effects of these antibacterial purine analogs. Compounds G2 and G14 failed to completely inhibit *B. subtilis* growth at analog concentrations up to 1 mM (data not shown), despite the fact that they caused more than 50% inhibition of cell growth at 100 μM (Figure 4, panel a).

Interestingly, many of the analogs, most notably G4 and G11, do not repress growth even though in-line probing assays indicate that these compounds can bind relatively tightly to a guanine riboswitch aptamer. There are several possible explanations for these observations. For example, these analogs may not enter bacterial cells to yield a concentration that is sufficient to inhibit riboswitch-mediated gene expression. If the compounds do enter cells by diffusion or by the action of purine transporters, they may be actively removed from cells by transporter protein activity (see further discussion below). Alternatively, compounds that do enter cells may be chemically modified such that the derivative compounds are no longer recognized by guanine riboswitches. Similarly, the compounds may be converted to natural intermediates in the purine metabolic pathway. In this case, repression of riboswitch-controlled genes may be irrelevant if the analog serves as a source for purine intermediates.

Gene regulation assays were performed to determine whether G6, G7 and G15 can repress the expression of a reporter gene controlled by a guanine riboswitch in *B. subtilis*. The 5′ UTR of the *B. subtilis xpt-pbuX* gene, including the endogenous promoter and riboswitch, was cloned upstream of a *lacZ* reporter gene, and the resulting construct was transformed into the *B. subtilis amyE* locus. A reporter construct in which the riboswitch is rendered incapable of regulating expression by mutation was also prepared. This construct carries three mutations that disrupt the P1 secondary structure element of the riboswitch aptamer and prevent guanine binding (construct M1 in reference 37). Reporter activity was then measured after adding each guanine analog at a concentration near its MIC.

β-galactosidase expression in the wild-type reporter strain is repressed by the addition of 200 μM guanine to the medium (Figure 4, panel c), whereas no repression is observed with the mutant strain under these conditions (Figure 4, panel d). In contrast, the addition of 3 μM G6 (75% of the MIC) does not repress reporter gene expression, even though bacterial growth is substantially slowed. Since the measured K_D for G6 *in vitro* is 3.3 μM, perhaps this analog does not accumulate inside bacteria at a sufficiently high concentration to trigger riboswitch function. More importantly, since G6 does not repress reporter gene expression at concentrations where growth inhibition occurs, its antimicrobial mechanism is probably not related to targeting guanine riboswitches.

At a concentration slightly below its MIC, G15 does reduce β-galactosidase expression by ~34%. However, repression is reduced to a similar extent in the strain containing an inactive riboswitch mutant, implying that reporter gene repression is not caused by G15-triggered riboswitch function. As with G6, G15 may inhibit bacterial growth through a mechanism that does not involve guanine riboswitches.

In contrast, significant repression of β-galactosidase activity occurs when the guanine analog G7 is added to the growth medium at concentrations near its MIC. Moreover, little repression is observed with the reporter strain carrying an inactive riboswitch variant, indicating that repression of reporter gene expression by G7 is likely mediated by the adjoining guanine riboswitch.

Analysis of *B. SUBTILIS* Strains that Overcome Inhibition by Guanine Analogs

In an effort to further understand the mechanisms by which G6, G7 and G15 inhibit growth, we sought to generate *B. subtilis* variants resistant to each analog. Wild-type *B. subtilis* strains were grown in the presence of the compounds at concentrations near their respective MICs, and serial inoculations of media with increasing analog concentrations were performed to generate resistant mutants. Using this method, attempts to generate G7- and G15-resistant *B. subtilis* mutant strains were unsuccessful because G7 and G15 become insoluble at concentrations only slightly higher than their respective MICs. However, four G6-resistant strains were isolated. The MICs were determined to be 125 μM for each of these mutant strains, corresponding to a 30-fold increase relative to the wild-type strain (Figure 4, panel b).

All four guanine riboswitches in each of the G6-resistant strains were sequenced and found to have no mutations. This finding is consistent with our data showing that G6 fails to

suppress a reporter gene controlled by a guanine riboswitch (Figure 4, panel c). As a control, we also sequenced the analogous adenine riboswitch (49) located upstream of the *pbuE* (formerly called *ydhL*) gene of the resistant *B. subtilis* strains. Adenine riboswitches form the same global aptamer architecture as do guanine riboswitches, but the RNA carries a key sequence difference in the ligand binding core that changes its specificity from guanine to adenine (37, 39, 49). Therefore, we initially expected that the adenine riboswitch would be far less likely than guanine riboswitches to acquire mutations that rendered bacteria resistant to guanine analogs. Surprisingly, each of the G6-resistant strains carried a mutation within the terminator stem of the expression platform for the *pbuE* adenine riboswitch (Figure 5).

In *B. subtilis*, the *pbuE* adenine riboswitch acts as a genetic ON switch that activates gene expression in response to adenine binding (49). Ligand binding by the riboswitch results in expression of a purine efflux pump that has been implicated in protection against toxic purine analogs (46). Among the four G6-resistant mutants, three possess distinct individual mutations within the *pbuE* riboswitch terminator, while the other mutant contains a large deletion that nearly eliminates the entire terminator stem (Figure 5). All of the single-nucleotide mutations are predicted to weaken terminator stem formation, which should favor activation of *pbuE* expression even in the absence of ligand binding by the adenine aptamer. Likewise, the loss of the terminator stem should maximally activate *pbuE* gene expression. These findings suggest that these mutants gain resistance to G6 by overexpressing a purine pump that rids the cell of the toxic guanine analog.

Interestingly, the large terminator stem deletion observed in this study has also been reported in another *B. subtilis* mutant resistant to the toxic purine analog 2-fluoroadenine (46), suggesting that *B. subtilis* cells may be particularly susceptible to this precise deletion mutation. In this regard it is notable that the five nucleotides immediately preceding the deleted segment (CAGGA) are identical in sequence to the last five nucleotides of the deleted segment. This sequence arrangement suggests that a DNA slippage event during DNA replication (53) may be unusually favorable in *B. subtilis*, leading us to identify a variant bacterium that is identical to a previously-reported variant that is known to resist inhibitory purine analogs (46).

Using the resistance generation method described above, we also isolated G6-resistant bacteria beginning with a *B. subtilis* strain wherein the *pbuE* gene was disrupted. The resulting G6-resistant bacteria still do not carry mutations within any of the guanine riboswitch regions, again suggesting that the antimicrobial effect of G6 does not involve riboswitch binding. Although we did not further pursue mapping of resistance mutations, one possible target of G6 is bacterial DNA polymerase IIIc, since several other C2-benzylated nucleobases are known to block DNA replication by inhibiting this enzyme (54).

G7 May be Targeting Guanine Riboswitches in *B. SUBTILIS*

G7 is the only analog examined in this study that binds to a guanine riboswitch aptamer *in vitro*, inhibits *B. subtilis* growth, and represses expression of a reporter gene that is controlled by a guanine riboswitch. In addition, the MIC values for G7 in all of the G6-resistant strains generated from either wild-type cells (Figure 4, panel b) or from cells carrying the *pbuE* deletion (data not shown) are no different from the MIC established for

wild-type. These results could be rationalized if G7 is not recognized by the PbuE transporter in G6-resistant cells carrying mutations to the *pbuE* adenine riboswitch. Furthermore, mutations in the *pbuE* deletion strain that render cells resistant to G6 must also have no effect on the mechanism for G7 activity, which could be explained if G7 indeed inhibits bacterial growth by binding riboswitches.

To further investigate the action of G7, various concentrations of G7 were added to media inoculated with the *B. subtilis* strain carrying the *xpt* riboswitch fused to a *lacZ* reporter gene as described earlier. We found that the concentration of G7 needed to fully repress reporter gene expression was 260 μM (Figure 6), which is the same as the concentration required for complete growth inhibition (Figure 4, panel b). This finding suggests that G7 may be inhibiting bacterial growth by binding to guanine riboswitches and repressing purine biosynthesis and/or transport genes.

The concentration of 260 μM G7 in the medium required to fully bring about cell growth inhibition and gene repression is more than 1000-fold higher than the K_D value measured for this compound binding to the *xpt* riboswitch aptamer (Figure 3, panel a). However, there are several possible explanations for this difference. For example, it is not known if the concentration of G7 added to the medium accurately reflects the concentration of the compound in bacteria. The cell could restrict entry of the compound, expel the compound if it enters the cell, or chemically modify the compound to change its ability to affect riboswitch function.

There are also several reasons why the function of the riboswitch may cause the difference between the values for MIC and K_D. For example, K_D values for aptamers are typically conducted with the aptamers in isolation from their adjoining expression platforms or other flanking nucleotides. Minimal aptamer constructs are likely to explore fewer alternative folding conformers that may involve nucleotides critical for ligand binding. Indeed, some aptamer constructs carrying flanking regions have been shown to have weaker ligand binding affinities compared to their minimized variants (*e.g.* see 22, 55). Given that the riboswitch RNA is being actively transcribed during the time it is sensing its ligand and controlling gene expression, the actual K_D value may vary with the elongation state of the 5′ UTR. Furthermore, it has been shown that some riboswitches function as kinetically-driven switches, rather than reaching thermodynamic equilibrium (40, 55–58). For riboswitches that terminate transcription using intrinsic terminator stems, such as the *xpt* representative, the concentration of ligand needed to efficiently trigger riboswitch function may be much higher than the K_D value measured *in vitro*.

Conclusions

Our survey of the functions of 16 guanine analogs designed to bind guanine riboswitches reveals several important issues that may be considered by those who seek to create antimicrobial compounds that target riboswitches. Like many other riboswitch classes, guanine riboswitches carry a well-conserved aptamer that is very specific for its ligand. The RNA almost entirely engulfs guanine, and uses every non-carbon atom on the purine ring as a point of recognition. This creates a binding pocket that discriminates against a great diversity of purine analogs (37). Despite the selectivity of the aptamer's binding pocket, we

have made use of the atomic-resolution structures of guanine riboswitch aptamers (38, 39) to create a series of analogs that are biased in favor of tight binding

It is likely that analogs could be designed that bind even more tightly to the aptamer by taking advantage of new interactions between the analog and functional groups of the aptamer that reside near the natural binding pocket. New tight-binding analogs also could be created that take advantage of structural rearrangements at the binding site, although these movements and interactions would be more difficult to predict only using the static structures derived from x-ray data. Even analogs more closely related to pyrimidines have been shown to be bound by a guanine riboswitch (59). These findings demonstrate that considerable chemical space has yet to be explored in the search for compounds that may bind and trigger guanine riboswitch function.

Similar rational design strategies should be applicable to other riboswitch classes when atomic-resolution structures become available. Currently, the three-dimensional structures of nine major classes of metabolite-binding riboswitches have been published (23–25, 34, 38, 39, 60–69). Some of these riboswitches control essential genes or multiple genes in various bacterial species, making them intriguing potential antibacterial targets (21). The availability of these atomic-resolution structures should allow researchers to assess space constraints within the binding pockets (70) and to identify analogs of the natural ligands that should retain binding and riboswitch triggering activities.

Although our collection of compounds is enriched for riboswitch binding activity *in vitro*, only about a third of the compounds are able to inhibit bacterial growth. In *B. subtilis*, guanine riboswitches control a collection of genes (Figure 1, panel b) that together appear essential for robust bacterial growth (Figure 1, panel c). Therefore, the low correspondence between riboswitch binding and bacterial growth inhibition is unlikely to be due to a problem with *B. subtilis* guanine riboswitches as targets for antimicrobial compounds. Rather, many other factors such as bioavailability and stability of the compound are likely involved in determining whether a riboswitch-binding analog will repress bacterial growth.

Based on MICs, the two compounds that are most effective at inhibiting bacterial growth are G6 and G7. Unfortunately, G6 does not repress the expression of a guanine riboswitch-controlled reporter gene in *B. subtilis* when the compound is present near its MIC. Therefore, G6 likely inhibits cell growth by a mechanism that does not involve guanine riboswitch binding. In contrast, G7 strongly represses guanine riboswitch-controlled reporter gene expression at a concentration that matches its MIC. However, this observation alone does not provide conclusive proof that the antibacterial activity of G7 is mediated exclusively by its action on guanine riboswitches. It is possible that G7 inhibits bacterial growth by associating with other targets in bacteria, or perhaps these other targets work synergistically with riboswitch-mediated gene inhibition to prevent bacterial growth.

G7 (6-*N*-hydroxylaminopurine) is a known mutagen in certain bacteria, as well as some yeast and mammalian cells (71, 72). It is thought that G7 can be converted to deoxyguanosine-5′-triphosphate in cells, and thus become incorporated into DNA during replication (73). However, many organisms (including some bacteria) are able to protect

themselves against the effects of the compound (73, 74). G7 has low potency in GMM and this potency decreases in rich medium (LB). Although the action of G7 suggests that guanine riboswitches can be made to serve as targets for antibacterial agents, new guanine analogs must be examined to create compounds that exhibit more drug-like properties. *B. subtilis* is not known to cause disease, and therefore the efficacy of antimicrobial compounds that target riboswitches in pathogenic bacteria should be evaluated to further ascertain clinical relevance. Even though guanine riboswitch distribution is not widespread in pathogens, the presence of representatives of this riboswitch class in key pathogens such as *B. anthracis* and *S. aureus* may offer opportunities to employ drugs that target this riboswitch class.

METHODS

Guanine Analogs

G4 was purchased from TCI Inc. G10 was purchased from Cheminpharma. G1 (75) and G11 (76) were synthesized as described previously. Other purine analogs were synthesized from 2-bromohypoxanthine or 2-amino-6-chloropurine precursors (Sigma-Aldrich) using methods similar to those described previously (76). Specifically, halopurine (2-bromohypoxanthine or 2-amino-6-chloropurine, 1 mmol) and the corresponding amine or hydrazine (3 mmol) were heated at 95°C for 3 hours in either dry methoxyethanol (G2, G3, G7, G8, G9, G14, G15, and G16) or methoxylethanol: water 3:1 (G5, G6, G12, G13, G16, and G17). After cooling to room temperature, each reaction was diluted with ethyl acetate and filtered through a scintered glass funnel to give the product, which was subsequently washed with ethyl acetate, water, and ethanol.

Guanine analogs were purified using an Agilent Technologies 1200 series HPLC with an Agilent Eclipse XDB-C18 column (5 micron; 250 mm length and 9.4 mm internal diameter) using a gradient of water/acetonitrile/trifluoroacetic acid (95/5/0.01 v/v/v) to acetonitrile/ trifluoroacetic acid (100/0.01 v/v). The purity of each compound was confirmed as greater than 95% by analytical HPLC with an Agilent Eclipse XDB-C18 column (5 micron; 75 mm length and 4.6 mm internal diameter) using a gradient of acetonitrile in water with 0.01% trifluoroacetic acid and detection at 254 nm and 210 nm wavelengths. Compounds typically eluted between 5% and 25% acetonitrile. The identities of the compounds were confirmed with ^{1}H-NMR and mass spectroscopy: (G1) ^{1}H NMR (500 MHz, DMSO-d_6): δ 8.13 (s, 1H); HRMS (ES) calculated for $C_6H_3F_3N_4O$: 204.0259. Found (MH+): 205.0486; (G2) ^{1}H NMR (500 MHz, DMSO-d_6): δ 3.69 (s, 3H), 8.31 (s, 1H), 11.5 (br, s, 1H); HRMS (EI) calculated for $C_6H_7N_5O_2$: 181.0600. Found (M+): 181.0602; (G3) ^{1}H NMR (500 MHz, DMSO-d_6): δ 4.88 (s, 3H), 7.25–7.43 (m, 3H), 7.43–7.51 (m, 2H), 7.82 (br s, 1H), 9.90 (br, s, 1H), 11.05 (br, s, 1H). HRMS (ES) calculated for $C_{12}H_{11}N_5O_2$: 257.0913. Found (M-H)$^-$: 256.0833; (G5) ^{1}H NMR (500 MHz, DMSO-d_6): δ 2.51 (s, 3H), 5.01 (br, s, 2H), 7.89 (br, s, 1H), 9.91 (br, s, 1H); HRMS (ES) calculated for $C_6H_8N_6O$: 180.0760. Found (MH+): 181.0830; (G6) ^{1}H NMR (500 MHz, DMSO-d_6): δ 6.73 – 6.77 (m, 3H), 7.15 – 7.19 (m, 2H), 7.87 (br, s, 1H), 8.20 (br, s, 1H), 8.90 (br, s, 1H), 10.90 (br, s, 1H). HRMS (ES) calculated for $C_{11}H_{10}N_6O$: 242.0916. Found (M-H)$^-$: 241.0836; (G7) ^{1}H NMR (500 MHz, DMSO-d_6): δ 6.50 (s, 2H), 7.69 (br, s, 1 H), 9.66 (br, s, 1H); HRMS (ES) calculated for $C_5H_6N_6O$:

166.0603. Found (M-H)$^-$: 165.0520; (G8) ^{1}H NMR (500 MHz, DMSO-d$_6$): δ 3.77 (s, 3H), 6.81 (br, s, 2H), 7.89 (br, s, 1H). HRMS (ES) calculated for $C_6H_8N_6O$: 180.0760. Found (M-H)$^-$: 179.0688; (G9) ^{1}H NMR (500 MHz, DMSO-d$_6$): δ 4.83 (s, 2H), 7.09–7.34 (m, 7H), 7.80 (br, s, 1H), 10.35 (br, 1H), 13.00 (br, 1H); HRMS (ES) calculated for $C_{12}H_{12}N_6O$: 256.1073. Found (MH+): 257.3022; (G10) ^{1}H NMR (400 MHz, DMSO-d$_6$): 5.80 (br, S, 2H), 6.60 (d, 2H), 7.70–7.80 (d, 3H), 9.0 (s, 1H), 9.15 (S, 1H), 12.2 (br, S, 1H); LRMS (ES) calculated for $C_{11}H_{10}N_6O$: 242.1. Found (MH+): 243.8; (G11) ^{1}H NMR (500 MHz, D_2O): δ 7.56 (s, 1H); HRMS (ES) calculated for $C_5H_7N_7$: 165.0763; Found (MH+): 166.2352; (G12) ^{1}H NMR (500 MHz, DMSO-d$_6$): δ 3.44 (s, 3H), 6.53 (br, s, 2H), 7.90 (s, 1H); HRMS (ES) calculated for $C_6H_{10}N_7$: 180.0998; Found (MH+): 181.0974; (G13) ^{1}H NMR (500 MHz, DMSO-d$_6$): δ 5.2 (s, 2H) 7.25 – 7.31 (m, 1H), 7.32 – 7.36 (m. 3H), 7.91 (br s, 1H). HRMS (EI) calculated for $C_{12}H_{13}N_7$: 255.1232. Found (M+): 255.1230; (G14) ^{1}H NMR (500 MHz, DMSO-d$_6$): δ 6.48 (s, 1H), 7.23 (t, *J* = 8 Hz, 2H), 7.42 (t, *J* = 8 Hz, 2H), 7.63 (d, 2H), 8.01 (s, 1H). HRMS (ES) calculated for $C_{11}H_{11}N_7$: 241.1076. Found (M-H)$^-$: 240.1000; (G15) ^{1}H NMR (500 MHz, DMSO-d$_6$): δ 3.79 (s, 3H), 6.98–7.01 (m, 2H), 7.52 (br, s, 1H), 7.72–7.76 (m, 2H), 8.26 (S, 1H), 10.45 (s, 1H). HRMS (EI) calculated for $C_{12}H_{12}N_6O$ 256.1073. Found (M+) 256.1072; (G16) ^{1}H NMR (500 MHz, DMSO-d$_6$): δ 3.00 (t, *J* = 4 Hz, 4H), 3.72 (t, *J* = 4 Hz, 4H), 6.80 (d, *J* = 8 Hz, 2H), 7.73 (d, *J* = 8 Hz, 2H), 8.84 (s, 1H), 12.13 (s, 1H); HRMS (ES) calculated for $C_{15}H_{17}N_7O$: 311.1495; Found (MH +): 312.1862.

B. SUBTILIS Gene Knockouts and Growth Assays

Four plasmid constructs were prepared via double-crossover to disrupt expression of the four guanine riboswitch-controlled genes (or operons) in *B. subtilis*. Regions homologous to fragments of *nupG*, *pbuG*, *xpt-pbuX*, and the *pur* operon were placed into pDG647, a modified pMXL3 (spectinomycin resistant marker, no xylose-inducible promoter) (35), pDG1515, and pMXL3, respectively. These four vectors were systematically transformed into *B. subtilis* strain 1A1, and in most cases this transformation integrated an antibiotic resistance cassette into the *B. subtilis* genome in place of the targeted gene. In the case of pMXL3, the entire *pur* operon was left intact but placed under a xylose-inducible promoter.

Overnight cultures (in LB) of this strain and a 1A1 wild-type strain were diluted to an OD_{600} of 0.1 in Mueller-Hinton broth (beef extract, 2 g L^{-1}, casein hydrolysate, 17.5 g L^{-1}, starch, 1.5 g L^{-1}) and grown for another hour. The cultures were centrifuged for 10 minutes at 2500 rpm, and pellets were resuspended and diluted to an OD_{600} of 0.3 in chemically defined glucose-minimal medium (GMM) (0.5% w/v glucose, 2 g L^{-1} $(NH_4)_2SO_4$, 14 g L^{-1} K_2HPO_4, 6 g L^{-1} KH_2PO_4, 1 g L^{-1} sodium citrate, 0.2 g L^{-1} $MgSO_4{\cdot}7H_2O$, 5 μM $MnCl_2$, 0.5 mM $CaCl_2$, 2.5 mM $MgCl_2$, 50 μg mL^{-1} tryptophan). In a 96-well plate, 50 μl of culture was added to 50 μl GMM. The entire plate was sealed with breathable film (USA Scientific) and incubated at 37°C with shaking. The absorbance was measured at 600 nm every hour for 13 hours to evaluate bacterial growth.

In-line Probing

A 90 nucleotide *xpt-pbuX* RNA construct encompassing the guanine riboswitch aptamer (Figure 1, panel a) was synthesized using a DNA template obtained from colony PCR of *B.*

subtilis strain 1A1. *In vitro* transcription followed by desphosphorylation and 5′ ^{32}P labeling was conducted as described previously (32) to produce RNA for in-line probing with different guanine analogs. Denaturing (8 M urea) 10% PAGE followed by analysis using a Molecular Dynamics Phosphorimager were used to establish RNA spontaneous cleavage patterns. In-line probing with increasing concentrations of each analog was used to assess binding affinities. The amount of RNA structural modulation was quantified as described previously (32) to estimate K_D values.

Antibacterial Assays

To measure the inhibitory effects of guanine analogs on bacterial growth, an overnight culture of *B. subtilis* 168 strain 1A1 in GMM was diluted by a factor of 100 and supplemented with the indicated analog at a final concentration of 100 μM. After growing for 10 hours at 37 °C with shaking, OD_{600} of the culture was measured and compared to that of the control culture where the medium was supplemented with only the corresponding solvent for the analog. The solvent was 100:5 dimethyl sulfoxide: 10 N NaOH (v/v) for G11, and was dimethyl sulfoxide for all other compounds. The MIC of each guanine analog was determined by growing a 1A1 *B. subtilis* strain overnight in LB, then diluting the culture into an OD_{600} of 0.1 in LB or GMM as noted. Guanine analog was added at various concentrations, the absorbance at 600 nm was monitored over time, and the MIC was calculated using the Clinical and Laboratory Standards Institute (CLSI) guidelines (77).

Reporter Gene Assays

A construct encompassing the entire *xpt-pbuX* guanine riboswitch or the M1 version of the riboswitch (37) was placed in a pDG1661 plasmid upstream of a β-galactosidase reporter gene. This vector was transformed into the *amyE* locus of *B. subtilis* strain 1A1, and β-galactosidase expression after the addition of various guanine analogs was measured using standard Miller assays as previously described (31).

Generation of G6-resistant Mutants

B. subtilis strain 1A1 was grown with shaking at 37°C in GMM with G6 added at the MIC (3.9 μM). When saturation of growth was reached, 10 mL culture was transferred into a culture tube containing 1 mL GMM with G6 added to a final concentration that was two-fold above the MIC (7.8 μM). This procedure was conducted four times, with the G6 concentration doubling with each serial passage, so that the final G6 concentration was 62.4 μM. The culture was plated onto LB, and DNA from the resulting colonies was isolated and used as a template to amplify the four guanine riboswitches and one adenine riboswitch found in *B. subtilis*. The resulting amplicons were sequenced to determine whether mutations were present. This experiment was repeated four times to discover several different mutations.

Acknowledgments

We thank members of the Breaker laboratory for helpful discussions. This work was supported by NIH award U54AI57158 (Northeast Biodefense Center--Lipkin) and by NIH grants (R33 DK07027 and GM 068819) to R.R.B. J.N.K. is a recipient of a predoctoral fellowship from the National Science Foundation. Research in the Breaker laboratory is also supported by the Howard Hughes Medical Institute.

K.F.B. and R.R.B. are cofounders of BioRelix, a company that is pursuing intellectual property related to the use of riboswitches as drug targets.

References

1. Walsh C. Molecular mechanisms that confer antibacterial drug resistance. Nature. 2000; 406:775–781. [PubMed: 10963607]
2. Theuretzbacher U, Toney JH. Nature's clarion call of antibacterial resistance: are we listening? Curr Opin Investig Drugs. 2006; 7:158–166.
3. Wolfson W. Holding back the tide of antibiotic resistance. Chem Biol. 2006; 13:1–3. [PubMed: 16426963]
4. Levy SB. The challenge of antibiotic resistance. Sci Am. 1998; 275:46–53. [PubMed: 9487702]
5. D'Costa VM, McGrann KM, Hughes DW, Wright GD. Sampling the antibiotic resistome. Science. 2006; 311:374–377. [PubMed: 16424339]
6. Bermingham A, Derrick JP. The folic acid biosynthesis pathway in bacteria: evaluation of potential for antibacterial drug discovery. Bioessays. 2002; 24:637–648. [PubMed: 12111724]
7. Koch AL. Bacterial wall as target for attack: past, present, and future research. Clin Microbiol Rev. 2003; 16:673–687. [PubMed: 14557293]
8. Maxwell A. DNA gyrase as a drug target. Trends Microbiol. 1997; 5:102–109. [PubMed: 9080608]
9. Poehlsgaard J, Douthwaite S. The bacterial ribosome as a target for antibiotics. Nat Rev Microbiol. 2005; 3:870–881. [PubMed: 16261170]
10. Majdalani N, Vanderpool CK, Gottesman S. Bacterial small RNA regulators. Crit Rev Biochem Mol Biol. 2005; 40:93–113. [PubMed: 15814430]
11. Mandal M, Breaker RR. Gene regulation by riboswitches. Nat Rev Mol Cell Biol. 2004; 5:451–463. [PubMed: 15173824]
12. Soukup JK, Soukup GA. Riboswitches exert genetic control through metabolite-induced conformational change. Curr Opin Struct Biol. 2004; 14:344–349. [PubMed: 15193315]
13. Winkler WC, Breaker RR. Regulation of bacterial gene expression by riboswitches. Annu Rev Microbiol. 2005; 59:487–517. [PubMed: 16153177]
14. Coppins RL, Hall KB, Groisman EA. The intricate world of riboswitches. Curr Opin Microbiol. 2007; 10:176–181. [PubMed: 17383225]
15. Montange RK, Batey RT. Riboswitches: emerging themes in RNA structure and function. Annu Rev Biophys. 2008; 37:117–133. [PubMed: 18573075]
16. Sudarsan N, Barrick JE, Breaker RR. Metabolite-binding RNA domains are present in the genes of eukaryotes. RNA. 2003; 9:644–647. [PubMed: 12756322]
17. Bocobza S, Adato A, Mandel T, Shapira M, Nudler E, Aharoni A. Riboswitch-dependent gene regulation and its evolution in the plant kingdom. Genes Dev. 2007; 21:2874–2879. [PubMed: 18006684]
18. Cheah MT, Wachter A, Sudarsan N, Breaker RR. Control of alternative RNA splicing and gene expression by eukaryotic riboswitches. Nature. 2007; 447:497–500. [PubMed: 17468745]
19. Croft MT, Moulin M, Webb ME, Smith AG. Thiamine biosynthesis in algae is regulated by riboswitches. Proc Natl Acad Sci USA. 2007; 104:20770–20775. [PubMed: 18093957]
20. Wachter A, Tunc-Ozdemir M, Grove BC, Green PJ, Shintani DK, Breaker RR. Riboswitch control of gene expression in plants by splicing and alternative 3′ end processing of mRNAs. Plant Cell. 2007; 19:3437–3450. [PubMed: 17993623]
21. Blount KF, Breaker RR. Riboswitches as antibacterial drug targets. Nat Biotechnol. 2006; 24:1558–1564. [PubMed: 17160062]
22. Winkler W, Nahvi A, Breaker RR. Thiamine derivatives bind messenger RNAs directly to regulate bacterial gene expression. Nature. 2002; 419:952–956. [PubMed: 12410317]
23. Edwards TE, Ferré-D'Amaré AR. Crystal structures of the thi-box riboswitch bound to thiamine pyrophosphate analogs reveal adaptive RNA-small molecule recognition. Structure. 2006; 14:1459–1468. [PubMed: 16962976]

24. Serganov A, Polonskaia A, Phan AT, Breaker RR, Patel DJ. Structural basis for gene regulation by a thiamine pyrophosphate-sensing riboswitch. Nature. 2006; 441:1167–1171. [PubMed: 16728979]
25. Thore S, Leibundgut M, Ban N. Structure of the eukaryotic thiamine pyrophosphate riboswitch with its regulatory ligand. Science. 2006; 312:1208–1211. [PubMed: 16675665]
26. Robbins WJ. The pyridine analog of thiamin and the growth of fungi. Proc Natl Acad Sci USA. 1941; 27:419–422. [PubMed: 16578020]
27. Woolley DW, White AGC. Selective reversible inhibition of microbial growth with pyrithiamine. J Exp Med. 1943; 78:489–497. [PubMed: 19871344]
28. Kawasaki T, Sanemori H, Egi Y, Yoshida S, Yamada K. Biochemical studies of pyrithiamine-resistant mutants of *Escherichia coli* K12. J Biochem. 1976; 79:1035–1042. [PubMed: 783154]
29. Kubodera T, Yamshita N, Nishimura A. Pyrithiamine resistance gene (ptrA) of *Aspergillus oryzae*: cloning, characterization and application as a dominant selectable marker for transformation. Biosci Biotechnol Biochem. 2000; 64:1416–1421. [PubMed: 10945258]
30. Sudarsan N, Cohen-Chalamish S, Nakamura S, Emilsson GM, Breaker RR. Thiamine pyrophosphate riboswitches are targets for the antimicrobial compound pyrithiamine. Chem Biol. 2005; 12:1325–1335. [PubMed: 16356850]
31. Sudarsan N, Wickiser JK, Nakamura S, Ebert MS, Breaker RR. An mRNA structure in bacteria that controls gene expression by binding lysine. Genes Dev. 2003; 1:2688–2697. [PubMed: 14597663]
32. Blount KF, Wang JX, Lim J, Sudarsan N, Breaker RR. Antibacterial lysine analogs that target lysine riboswitches. Nat Chem Biol. 2006; 3:44–49. [PubMed: 17143270]
33. Ataide SF, Wilson SN, Dang S, Rogers TE, Roy B, Banerjee R, Henkin TM, Ibba M. Mechanisms of resistance to an amino acid antibiotic that targets translation. ACS Chem Biol. 2007; 2:819–827. [PubMed: 18154269]
34. Serganov A, Huang L, Patel DJ. Molecular insights into coenzyme recognition and gene regulation by a FMN riboswitch. Nature. 2009; 458:233–237. [PubMed: 19169240]
35. Lee ER, Blount KF, Breaker RR. Roseoflavin is a natural antibacterial compound that binds to FMN riboswitches and regulates gene expression. RNA Biol. 2009 (in press).
36. Ott E, Stolz J, Lehmann M, Mack M. The RFN riboswitch of Bacillus subtilis is a target for the antibiotic roseoflavin produced by Streptomyces davawensis. RNA Biol. 2009 (in press).
37. Mandal M, Boese B, Barrick JE, Winkler WC, Breaker RR. Riboswitches control fundamental biochemical pathways in *Bacillus subtilis* and other bacteria. Cell. 2003; 113:577–586. [PubMed: 12787499]
38. Batey RT, Gilbert SD, Montange RK. Structure of a natural guanine-responsive riboswitch complexed with the metabolite hypoxanthine. Nature. 2004; 432:411–415. [PubMed: 15549109]
39. Serganov A, Yuan YR, Pikovskaya O, Polonskaia A, Malinina L, Phan AT, Hobartner C, Micura R, Breaker RR, Patel DJ. Structural basis for discriminative regulation of gene expression by adenine- and guanine-sensing mRNAs. Chem Biol. 2004; 11:1729–1741. [PubMed: 15610857]
40. Gilbert SD, Stoddard CD, Wise SJ, Batey RT. Thermodynamic and kinetic characterization of ligand binding to the purine riboswitch aptamer domain. J Mol Biol. 2006; 359:754–768. [PubMed: 16650860]
41. Gilbert SD, Love CE, Edwards AL, Batey RT. Mutational analysis of the purine riboswitch aptamer domain. Biochemistry. 2007; 46:13297–13309. [PubMed: 17960911]
42. Mulhbacher J, Lafontaine DA. Ligand recognition determinants of guanine riboswitches. Nucleic Acids Res. 2007; 35:5568–5580. [PubMed: 17704135]
43. Stoddard CD, Gilbert SD, Batey RT. Ligand-dependent folding of the three-way junction in the purine riboswitch. RNA. 2008; 14:675–684. [PubMed: 18268025]
44. Lemay JF, Penedo JC, Tremblay R, Lilley DM, Lafontaine DA. Folding of the adenine riboswitch. Chem Biol. 2006; 13:857–868. [PubMed: 16931335]
45. Barrick JE, Breaker RR. The distributions, mechanisms, and structures of metabolite-binding riboswitches. Genome Biol. 2007; 8:R239. [PubMed: 17997835]

46. Johansen LE, Nygaard P, Lassen C, Agerso Y, Saxild HH. Definition of a second *Bacillus subtilis pur* regulon comprising the *pur* and *xpt-pbuX* operons plus *pbuG*, *nupG* (*yxjA*), and *pbuE* (*ydhL*). J Bacteriol. 2003; 185:5200–5209. [PubMed: 12923093]
47. Kobayashi K, et al. Essential *Bacillus subtilis* genes. Proc Natl Acad Sci USA. 2003; 100:4678–4683. [PubMed: 12682299]
48. Meisenzahl AC, Shapiro L, Jenal U. Isolation and characterization of a xylose-dependent promoter from *Caulobacter crescentus*. J Bacteriol. 1997; 173:592–600. [PubMed: 9006009]
49. Mandal M, Breaker RR. Adenine riboswitches and gene activation by disruption of a transcription terminator. Nat Struct Mol Biol. 2004; 11:29–35. [PubMed: 14718920]
50. Soukup GA, Breaker RR. Relationship between internucleotide linkage geometry and the stability of RNA. RNA. 1999; 5:1308–1325. [PubMed: 10573122]
51. Soukup GA, DeRose EC, Koizumi M, Breaker RR. Generating new ligand-binding RNAs by affinity maturation and disintegration of allosteric ribozymes. RNA. 2001; 7:524–536. [PubMed: 11345431]
52. Andrews JM. Determination of minimum inhibitory concentrations. J Antimicrob Chemther. 2001; 48:5–16.
53. Gore JM, Ran FA, Ornston LN. Deletion mutations caused by DNA strand slippage in *Acinetobacter baylyi*. Appl Environ Microbiol. 2006; 72:5239–5245. [PubMed: 16885271]
54. Wright GE, Brown NC, Xy WC, Long ZY, Zhi C, Gambino JJ, Barnes MH, Butler MM. Active site directed inhibitors of replication-specific bacterial DNA polymerases. Bioorg Med Chem Lett. 2005; 15:729–732. [PubMed: 15664846]
55. Wickiser JK, Winkler WC, Breaker RR, Crothers DM. The speed of RNA transcription and metabolite binding kinetics operate an FMN riboswitch. Mol Cell. 2005; 18:49–60. [PubMed: 15808508]
56. Wickiser JK, Cheah MT, Breaker RR, Crothers DM. The kinetics of ligand binding by an adenine-sensing riboswitch. Biochemistry. 2005; 44:13404–13414. [PubMed: 16201765]
57. Rieder R, Lang K, Graber D, Micura R. Ligand-induced folding of the adenosine deaminase A-riboswitch and implications on riboswitch translational control. Chembiochem. 2007; 8:896–902. [PubMed: 17440909]
58. Lang K, Rieder R, Micura R. Ligand-induced folding of the *thiM* TPP riboswitch investigated by a structure-based fluorescence spectroscopic approach. Nucleic Acids Res. 2007; 35:5370–5378. [PubMed: 17693433]
59. Gilbert SD, Mediatore SJ, Batey RT. Modified pyrimidines specifically bind purine the riboswitch. J Am Chem Soc. 2006; 128:14214–14215. [PubMed: 17076468]
60. Montange RK, Batey RT. Structure of the *S*-adenosylmethionine riboswitch regulatory element. Nature. 2006; 29:1172–1175. [PubMed: 16810258]
61. Klein DJ, Ferré-D'Amaré AR. Structural basis of *glmS* ribozyme activation by glucosamine-6-phosphate. Science. 2006; 313:1752–1756. [PubMed: 16990543]
62. Cochrane JC, Lipchock SV, Strobel SA. Structural investigation of the GlmS ribozyme bound to its catalytic cofactor. Chem Biol. 2007; 14:97–105. [PubMed: 17196404]
63. Gilbert SD, Rambo RP, Van Ryne D, Batey RT. Structure of the SAM-II riboswitch bound to *S*-adenosylmethionine. Nat Struct Mol Biol. 2008; 15:177–182. [PubMed: 18204466]
64. Lu C, Smith AM, Fuchs RT, Ding F, Rajashankar K, Henkin TM, Ke A. Crystal structures of the SAM-III/S(MK) riboswitch reveal the SAM-dependent translation inhibition mechanism. Nat Struct Mol Biol. 2008; 15:1076–1083. [PubMed: 18806797]
65. Garst AD, Heroux A, Rambo RP, Batey RT. Crystal structure of the lysine riboswitch regulatory mRNA element. J Biol Chem. 2008; 15:22347–22351. [PubMed: 18593706]
66. Serganov A, Huang L, Patel DJ. Structural insights into amino acid binding and gene control by a lysine riboswitch. Nature. 2008; 455:1263–1267. [PubMed: 18784651]
67. Kline DJ, Edwards TE, Ferré-D'Amaré AR. Cocrystal structure of a class I preQ$_1$ riboswitch reveals a pseudoknot recognizing an essential hybermodified nucleobase. Nat Struct Mol Biol. 2009; 16:343–344. [PubMed: 19234468]

68. Kang M, Peterson R, Feigon J. Structural insights into riboswitch control of the biosynthesis of queuosine, a modified nucleotide found in the anticodon of tRNA. Mol Cell. 2009; 33:784–790. [PubMed: 19285444]
69. Spitale RC, Torelli AT, Krucinska J, Bandarian V, Wedekind JE. The structural basis for recognition of the preQ$_0$ metabolite by an unusually small riboswitch aptamer domain. J Biol Chem. 2009; 284:11012–11016. [PubMed: 19261617]
70. Edwards TE, Klein DJ, Ferré-D'Amaré AR. Riboswitches: small-molecule recognition by gene regulatory RNAs. Curr Opin Struct Biol. 2007; 17:273–279. [PubMed: 17574837]
71. Barrett JC. Induction of gene mutation in and cell transformation of mammalian cells by modified purines: 2-Aminopurine and 6-*N*-hydroxylaminopurine. Proc Natl Acad Sci USA. 1981; 78:5685–5689. [PubMed: 6946507]
72. Pavlov YI, Noskov VN, Lange EK, Moiseeva EV, Pshenichnov MR, Khromov-Borisov NN. The genetic activity of N6-hydroxyadenine and 2-amino N6-hydroxyadenine in *Escherichia coli*, *Salmonella typhimurium* and *Saccharomyces cerevisiae*. Mutat Res. 1991; 253:33–46. [PubMed: 1870608]
73. Kozmin SG, Schaaper RM, Shcherbakova PV, Kulikov VN, Noskov VN, Guetsova ML, Alenin VV, Rogozin IB, Makarova KS, Pavlov YI. Multiple antimutagenesis mechanisms affect mutagenic activity and specificity of the base analog 6-*N*-hydroxylaminopurine in bacteria and yeast. Mutat Res. 1997; 402:41–50. [PubMed: 9675240]
74. Kozmin SG, Schaaper RM. Molybdenum cofactor-dependent resistance to *N*-hydroxylated base analogs in *Escherichia coli* is independent of MobA function. Mutat Res. 2007; 619:9–15. [PubMed: 17349664]
75. Giner-Sorolla A, Bendich A. Fluorine-containing pyrimidines and purines: synthesis and properties of trifluoromethyl pyrimidines and purines. J Am Chem Soc. 1958; 80:5744–5752.
76. Wright GE, Dudycz LW. Synthesis and characterization of N2-(p-n-butylphenyl)-2′-deoxyguanosine and its 5′-triphosphate and their inhibition of HeLa DNA polymerase alpha. J Med Chem. 1984; 27:175–181. [PubMed: 6694166]
77. Clinical and Laboratory Standards Institute. Methods for Dilution Antimicrobial Susceptibility Tests for Bacteria that Grow Aerobically: Approved Standards: M7-A7. National Committee for Clinical Laboratory Standards; Wayne, Pennsylvania, USA: 2006.
78. Saxild HH, Nygaard P. Genetic and physiological characterization of Bacillus subtilis mutants resistant to purine analogs. J Bacteriol. 1987; 169:2977–2983. [PubMed: 3110131]
79. Saxild HH, Brunstedt K, Nielsen KI, Jarmer H, Nygaard P. Definition of the *Bacillus subtilis* PurR operator using genetic and bioinformatic tools and expansion of the PurR regulon with *glyA*, *guaC*, *pbuG*, *xpt-pbuX*, *yqhZ-folD*, and *pbuO*. J Bacteriol. 2001; 183:6175–6183. [PubMed: 11591660]

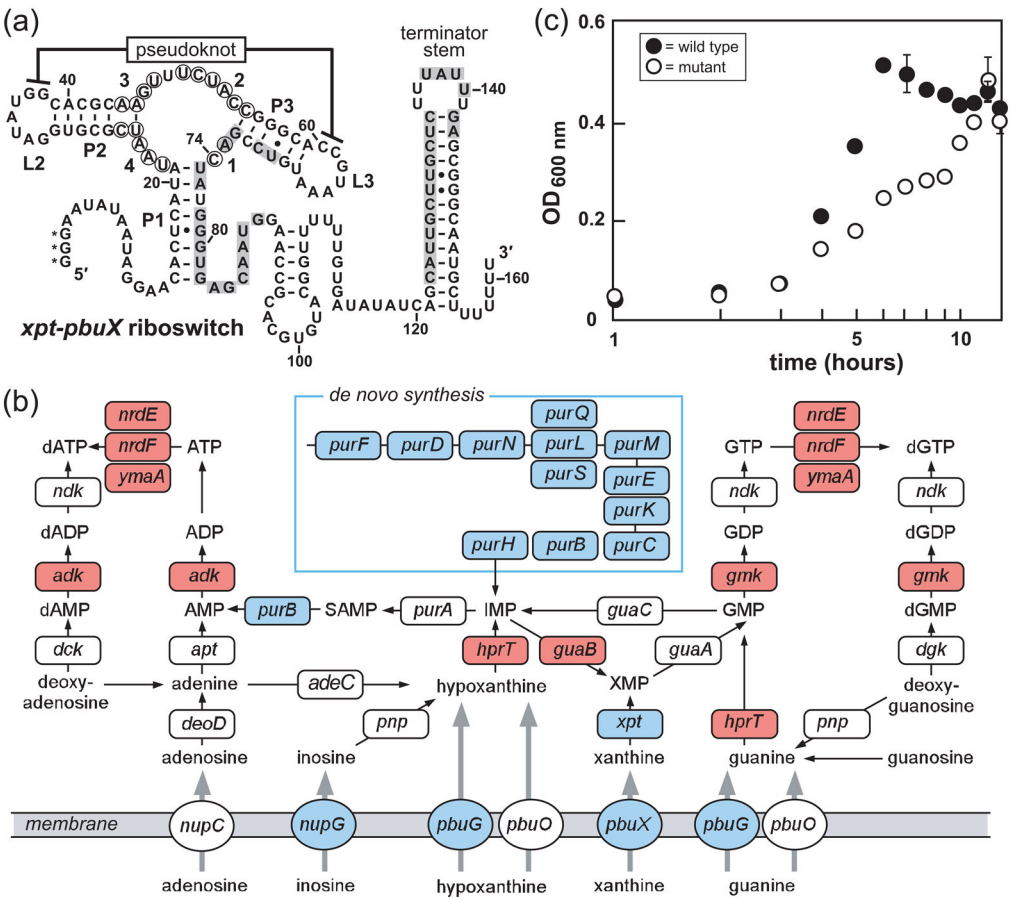

Figure 1.

Guanine riboswitches and guanine riboswitch-controlled genes in *B. subtilis*. a) Sequence and secondary structure of the *xpt-pbuX* guanine riboswitch from *B. subtilis*. Base-paired stems are denoted P1, P2 and P3, while loops are designated L2 and L3. Circled nucleotides identify those that undergo reduction of spontaneous cleavage during in-line probing reactions containing guanine concentrations above the K_D, and positions are numbered as in Fig. 3b. Shaded nucleotides identify alternative pairing for the formation of the putative anti-terminator stem that may form when ligand is absent. Asterisks indicate nucleotides added to the RNA sequence to facilitate synthesis when this construct was prepared by *in vitro* transcription. b) Purine metabolic pathways in *B. subtilis* (47, 78, 79). Genes essential for *B. subtilis* growth (47) are highlighted in red, genes regulated by guanine riboswitches (37) are depicted in blue. c) The effects of the disruption of all four guanine riboswitch-controlled transcriptional units in *B. subtilis*. Growth curves of a wild-type *B. subtilis* strain (wild type) and a strain with all guanine riboswitch-controlled genes disrupted (mutant) are shown. The mutant strain carries knockouts of the genes controlled by the *xpt-pbuX*, *pbuG*, *nupG* riboswitches, and carries the *pur* operon downstream of a xylose-inducible promoter. The average of three independent growth assays is shown. Error bars depict the standard deviation of three separate assays, and were not added when the error was less than the width of the points.

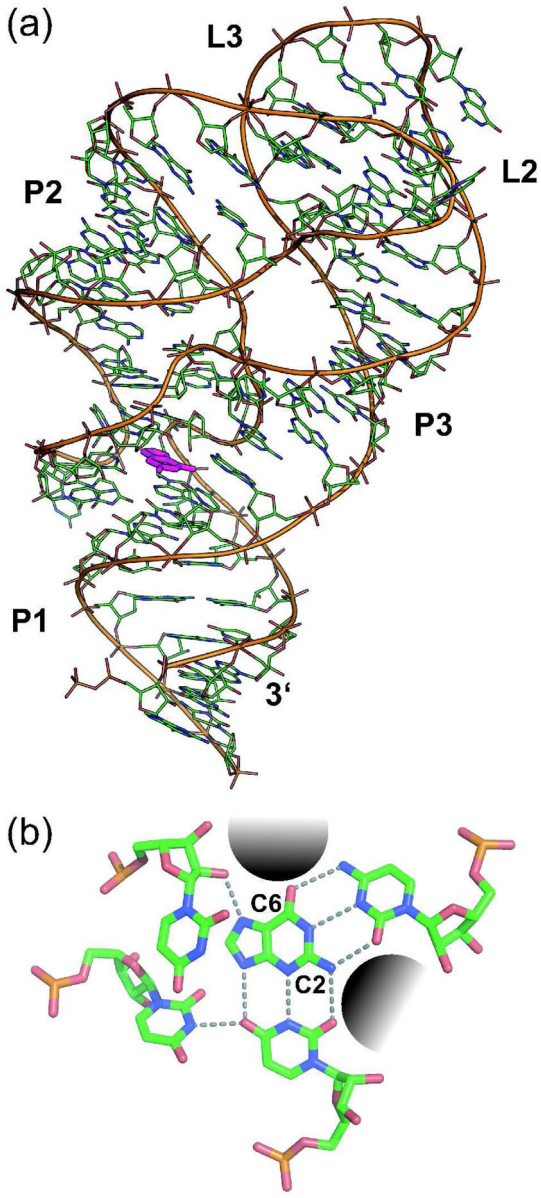

Figure 2.

Assessing ligand recognition by a riboswitch aptamer. a) Atomic-resolution structure of the *xpt* riboswitch aptamer bound to guanine (39). b) A close-up view of guanine in the binding pocket of the aptamer. Dashed lines designate hydrogen bonding interactions between nucleotides of the binding pocket and the guanine ligand (central base). The gray shaded areas (near C2 and C6 positions of guanine) highlight spaces where it may be possible to add different chemical groups without substantially disrupting binding to the aptamer.

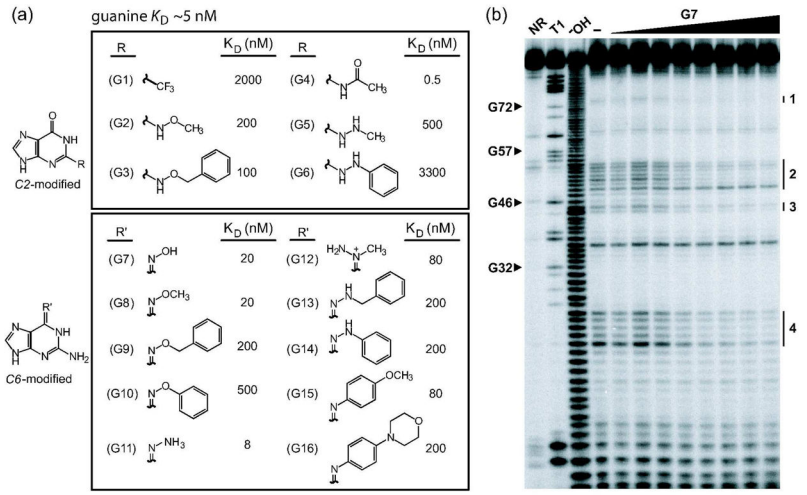

Figure 3.

Guanine analog design and the binding characteristics of guanine analogs by the *xpt-pbuX* riboswitch *in vitro*. a) Guanine analog structures and K_D values. The 16 guanine analogs are separated into two groups depending on whether chemical changes are made to the C2 or C6 position. b) PAGE analysis of the products of an in-line probing assay with the *xpt* aptamer (Figure 1, panel a). NR, T1, and $^{-}$OH designate 5′ ^{32}P-labeled RNAs subjected to no reaction, partial digest with RNase T1, or partial digestion with alkali, respectively. RNAs were incubated with G7 concentrations ranging from 0 to 1 μM, where (−) indicates incubation without ligand. Arrowheads identify several bands corresponding to nuclease cleavage after G residues (T1 lane) as designated according to the numbering system used in Figure 1, panel a. Regions 1 through 4 denote areas of structural modulation within the aptamer when ligand is bound.

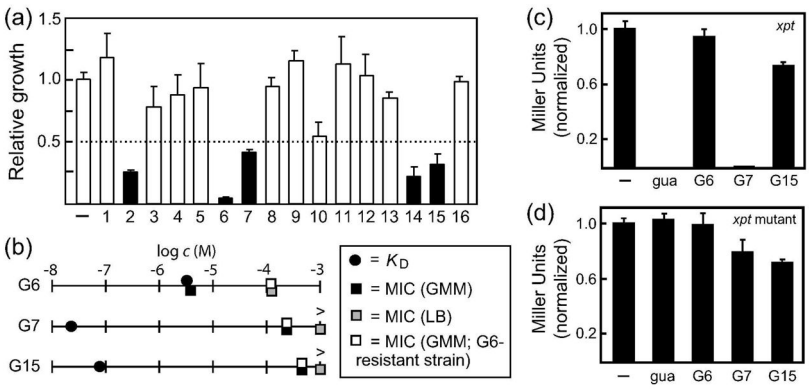

Figure 4.

Identification of guanine analogs that inhibit cell growth and repress reporter gene expression. a) Growth inhibition by guanine analogs. Each guanine analog was added to *B. subtilis* cultures to a final concentration of 100 μM, and the relative growth compared to that observed with no added analog (−) was determined after incubation for 10 hr at 37°C. The average growth for three independent cultures is shown, wherein open and filled bars identify analogs that inhibit bacterial growth less than or greater than 50%, respectively. Error bars represent the standard deviation between three independent assays. b) Plots comparing the K_D and MIC values for three guanine analogs. The MIC values for G6, G7 and G15. MIC (GMM) and MIC (LB) values were established using the wild-type 1A1 *B. subtilis* strain. MIC (G6-resistant strain, GMM) values were established using a 1A1 *B. subtilis* variant that was generated to exhibit resistance to G6 (the variant carrying the near complete deletion of the terminator stem of the *pbuE* riboswitch, see Figure 5). MIC values for G7 and G15 in rich medium were not detected even at 1 mM, as represented by the > symbol. C–d) Plots of β-galactosidase expression for the wild-type and mutant (M1; see Methods) *xpt-pbuX* constructs normalized to the level of expression observed without added ligand. The *xpt-pbuX* guanine riboswitch was placed upstream of a *lacZ* reporter gene in a wild-type *B. subtilis* strain, and each compound was added to this strain at 75% of the MIC for the compound, or 200 μM in the case of guanine. The annotations (−) and gua designate no added ligand and guanine, respectively. A normalized value of one equals 45 Miller units for the wild-type *xpt-pbuX* strain and 27 Miller units for the mutant *xpt-pbuX* strain.

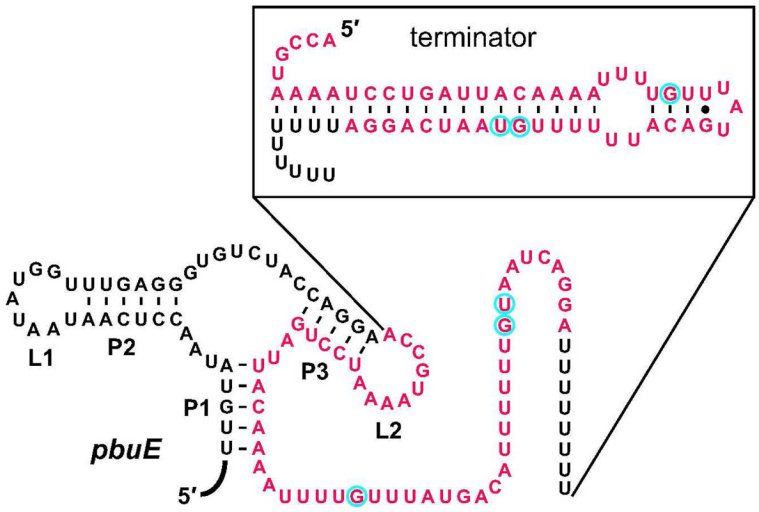

Figure 5.

Sequence and secondary structure of the *pbuE* adenine riboswitch in *B. subtilis*. In the absence of adenine, the riboswitch assembles a transcription terminator stem (shown in the box above). Lines from the box to the *pbuE* secondary structure designate the beginning and end points of the nucleotides shown in the box. The red nucleotides depict the deletion mutation found in one G6-resistant strain. The blue circles each represent one G6-resistant mutant strain in which the corresponding point mutation was found.

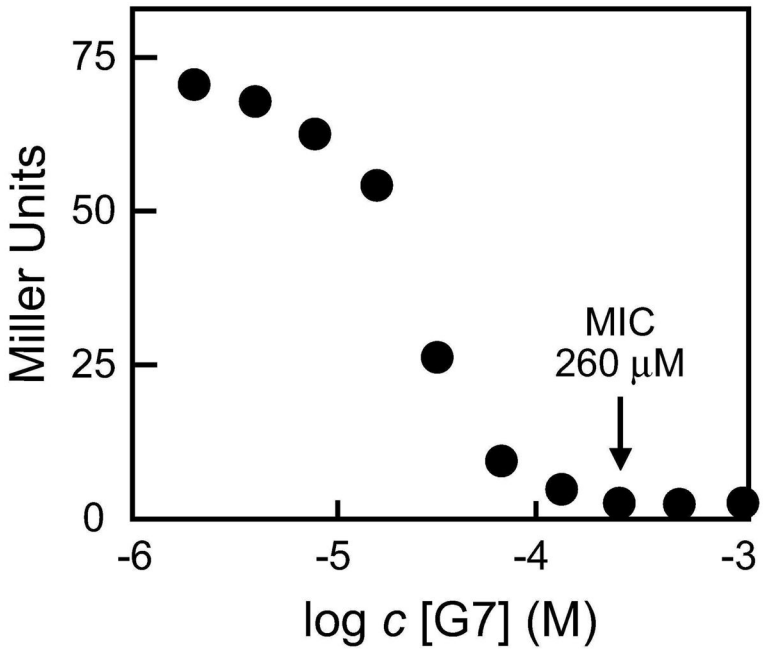

Figure 6.

Plot depicting β-galactosidase expression versus increasing concentrations of G7. The arrow depicts the concentration at which gene expression is approximately zero, which also corresponds to the MIC.